

RESEARCH ARTICLE



Oncogenic PKC- ι activates Vimentin during epithelial-mesenchymal transition in melanoma; a study based on PKC- ι and PKC- ζ specific inhibitors

Wishrawana S. Ratnayake^a, Christopher A. Apostolatos^{a,†}, André H. Apostolatos ^{a,†}, Ryan J. Schutte^b,
Monica A. Huynh^b, David A. Ostrov^b and Mildred Acevedo-Duncan^a

^aDepartment of Chemistry, University of South Florida, Tampa, FL, USA; ^bDepartment of Pathology, Immunology and Laboratory Medicine, University of Florida, College of Medicine, Gainesville, FL, USA

ABSTRACT

Melanoma is one of the fastest growing cancers in the United States and is accompanied with a poor prognosis owing to tumors being resistant to most therapies. Atypical protein kinase Cs (aPKC) are involved in malignancy in many cancers. We previously reported that aPKCs play a key role in melanoma's cell motility by regulating cell signaling pathways which induce epithelial-mesenchymal Transition (EMT). We tested three novel inhibitors; [4-(5-amino-4-carbamoylimidazol-1-yl)-2,3-dihydroxycyclopentyl] methyl dihydrogen phosphate (ICA-1T) along with its nucleoside analog 5-amino-1-((1R,2S,3S,4R)-2,3-dihydroxy-4-methylcyclopentyl)-1H-imidazole-4-carboxamide (ICA-1S) which are specific to protein kinase C- ι (PKC- ι) and 8-hydroxy-1,3,6-naphthalenetrisulfonic acid (ζ -Stat) which is specific to PKC- ζ on cell proliferation, apoptosis, migration and invasion of two malignant melanoma cell lines compared to normal melanocytes. Molecular modeling was used to identify potential binding sites for the inhibitors and to predict selectivity. Kinase assay showed >50% inhibition for specified targets beyond 5 μ M for all inhibitors. Both ICA-1 and ζ -Stat significantly reduced cell proliferation and induced apoptosis, while ICA-1 also significantly reduced migration and melanoma cell invasion. PKC- ι stimulated EMT via TGF β /Par6/RhoA pathway and activated Vimentin by phosphorylation at S39. Both ICA-1 and ζ -Stat downregulate TNF- α induced NF- κ B translocation to the nucleus there by inducing apoptosis. Results suggest that PKC- ι is involved in melanoma malignancy than PKC- ζ . Inhibitors proved to be effective under *in-vitro* conditions and need to be tested *in-vivo* for the validity as effective therapeutics. Overall, results show that aPKCs are essential for melanoma progression and metastasis and that they could be used as effective therapeutic targets for malignant melanoma.

ARTICLE HISTORY

Received 21 March 2018
Revised 20 April 2018
Accepted 25 April 2018

KEYWORDS

PKC- ι ; apoptosis; invasion; migration; metastasis; melanoma; vimentin

Introduction

Melanoma is a deadly skin cancer that develops in melanocytes. The rates of melanoma have been rising for the last 30 years. In 2017, 87,110 new melanoma cases and nearly 10,000 related deaths were reported [1]. Most available drugs target BRAF (V600E) mutation which occurs in ~60% melanoma cases, yet melanoma has a poor prognosis and tumors acquire resistance to BRAF mutation inhibition [2]. Currently available and FDA (U.S. Food and Drug Administration) approved combination therapies for advanced melanoma include dabrafenib + trametinib and vemurafenib + cobimetinib. These may improve survival, but they also pose adverse toxic effects [3,4]. The FDA approved only decarbazine as a chemotherapeutic drug for melanoma which has only 7–12% response rate [5].

We recently confirmed aPKCs as oncogenes and a potential therapeutic target for metastatic melanoma [6,7]. PKC- ι and PKC- ζ are overexpressed in melanoma cell lines compared to undetectable levels of PKC- ι and very low levels of PKC- ζ in normal melanocytes. We have also reported that aPKC inhibition may increase the level of E-cadherin and decrease the level of Vimentin suggesting that aPKC inhibition could slowdown EMT in melanoma. But the specific roles of PKC- ι and PKC- ζ have not been identified [6]. Selzer, et al. also reported that PKC- ι may play a role in cellular malignancy owing to its association with transform phenotypes of human melanoma both *in-vivo* and *in-vitro* [8]. In addition, PKC- ι and PKC- ζ are involved in tumorigenesis, progression and survival of many cancers. More specifically, PKC- ι is involved in rapid cell proliferation of human glioma cells, lung cancer

CONTACT Mildred Acevedo-Duncan, PhD  macevedo@usf.edu  Department of Chemistry, 4202 E Fowler Ave, CHE 205, Tampa, FL, 33620.

[†]These authors contributed equally to this work.

© 2018 The Author(s). Published by Informa UK Limited, trading as Taylor & Francis Group

This is an Open Access article distributed under the terms of the Creative Commons Attribution-NonCommercial-NoDerivatives License (<http://creativecommons.org/licenses/by-nc-nd/4.0/>), which permits non-commercial re-use, distribution, and reproduction in any medium, provided the original work is properly cited, and is not altered, transformed, or built upon in any way.

cells and neuroblastoma cells while PKC- ζ plays a role in malignancy of prostate cancer cells [9–12].

Our previous work on melanoma reported that aPKCs inhibition or knockdown of its expression could significantly induce apoptosis, reduce migration and invasion. Notably, we found increases in NF- κ B p65 levels upon inhibition of aPKCs, which we posited due to upstream signaling for NF- κ B translocation. NF- κ B translocation appears to be blocked upon inhibition of aPKCs, resulting in further NF- κ B accumulation in the cytoplasm [6].

PKC- ι was first considered as a novel therapeutic target by Stallings-Mann, et al. in 2006. They screened aurothiomalate as a potent inhibitor of the interaction between PB1 domain of PKC- ι and Par6 [13]. Half maximal inhibitory concentration (IC₅₀) of aurothiomalate ranged from 0.3–100 μ M and indicated that some cell lines are insensitive (i.e. H460 and A549 lung cancer cells) to the inhibitor [10]. Aurothiomalate has the potential risk of developing gold toxicity even with low levels of the inhibitor, which is a common problem with gold therapy in rheumatoid arthritis [14]. ICA-1T analog was reported by Pillai, et al. as novel potential inhibitor for PKC- ι in neuroblastoma cells in 2011 which demonstrated IC₅₀ as 0.1 μ M which was 1000 times less than aurothiomalate IC₅₀ on BE(2)-C neuroblastoma cells [11].

Vimentin is a type of intermediate filament and a highly dynamic structure that is essential for organizing actin and tubulin systems, changing cell polarity, and thereby changing cell motility and regulating cell signaling. Moreover, Vimentin plays a very important role in gaining rear-to-front polarity for mesenchymal cells, making it a hallmark of EMT. Vimentin phosphorylation regulates integrins which are needed for proper cell adhesion and invasion of cancer cells [15]. During activation, Vimentin's tail region binds to head region, resulting in phosphorylation at S39, leading to an increase in cancer cell motility and invasion (both *in-vitro* and *in-vivo*). Phosphorylation at S39 on Vimentin therefore indicates its activation. AKT and PKC- ϵ are known to activate Vimentin [15–17].

In the present study, we report the effects of a novel PKC- ζ specific inhibitor ζ -Stat and PKC- ι specific inhibitor ICA-1S on cell proliferation, apoptosis, migration and invasion on metastatic melanoma cells and normal melanocytes in comparison to ICA-1T. We place emphasis on determining the roles of aPKCs in melanoma cell signaling related to metastasis and report virtual screening of these inhibitors to identify their specific binding to the said proteins. When ICA-1T was first presented, PKC- ι crystal structure was not available, therefore a homology model was used [11]. In the present study, we used the PKC- ι crystal structure thereby increased the

accuracy of computational predictions. However, a SWISS-MODEL of PKC- ζ was used owing to the unavailability of the PKC- ζ crystal structure. Specificity of ζ -Stat is therefore heavily justified by experimental data. Here, we report that PKC- ι activates Vimentin intermediate assembly during EMT and it could possibly regulate the expression of Vimentin. We also report that both aPKCs induce cell survival via the AKT/NF- κ B pathway and PKC- ι induces cell migration and invasion via the Par6/RhoA and Smad 2/3 pathways. We also conducted tests to determine if TGF β and TNF- α stimulate the above pathways and found that TNF- α increased the levels of both PKC- ι and PKC- ζ and thereby increased the translocation of activated NF- κ B complex to the nucleus. TGF β stimulation significantly increased the levels of PKC- ι and Vimentin and thereby induced EMT in melanoma cells.

Results

Specific binding of ICA-1S, ICA-1T and ζ -Stat to PKC- ι and PKC- ζ allosteric binding pockets

Molecular docking of ICA-1T, ICA-1S, and ζ -Stat (Figures 1A, 1B & 1C) to structures of PKC- ι identified an allosteric binding pocket (Figures 1D & 1E). The pocket, located within the C-lobe of the kinase domain, is framed by solvent exposed residues of helices α F- α I and the activation segment [18]. The pocket is primarily composed of residues conserved between PKC- ι and PKC- ζ . Presence of this pocket was validated by Pillai, et al. using several biochemical assays [11]. As a means of determining whether ATP influences the drug binding, we compared molecular docking scores using structures of the ATP bound and unbound forms of PKC- ι . Molecular docking, using AutoDock Vina, suggested that the ICA-1S and ICA-1T have the potential to interact with PKC- ι in the presence and absence of ATP with high affinities (Table in Figure 1, part F).

Specific activities of ICA-1S, ICA-1T and ζ -Stat on PKC- ι and PKC- ζ

There is 70% similarity between the primary structures of PKC- ι and PKC- ζ catalytic domains, so it was essential to determine the specificity of inhibitors [19]. The specificity of ICA-1T was previously reported as inhibiting only PKC- ι without affecting other PKC isoforms [11]. In this case, we report for the first time that nucleoside analog (ICA-1S) also shows a significant specificity towards the same allosteric site of PKC- ι . Additionally, kinase activity shows that ζ -Stat is specific to PKC- ζ only which proves the molecular docking

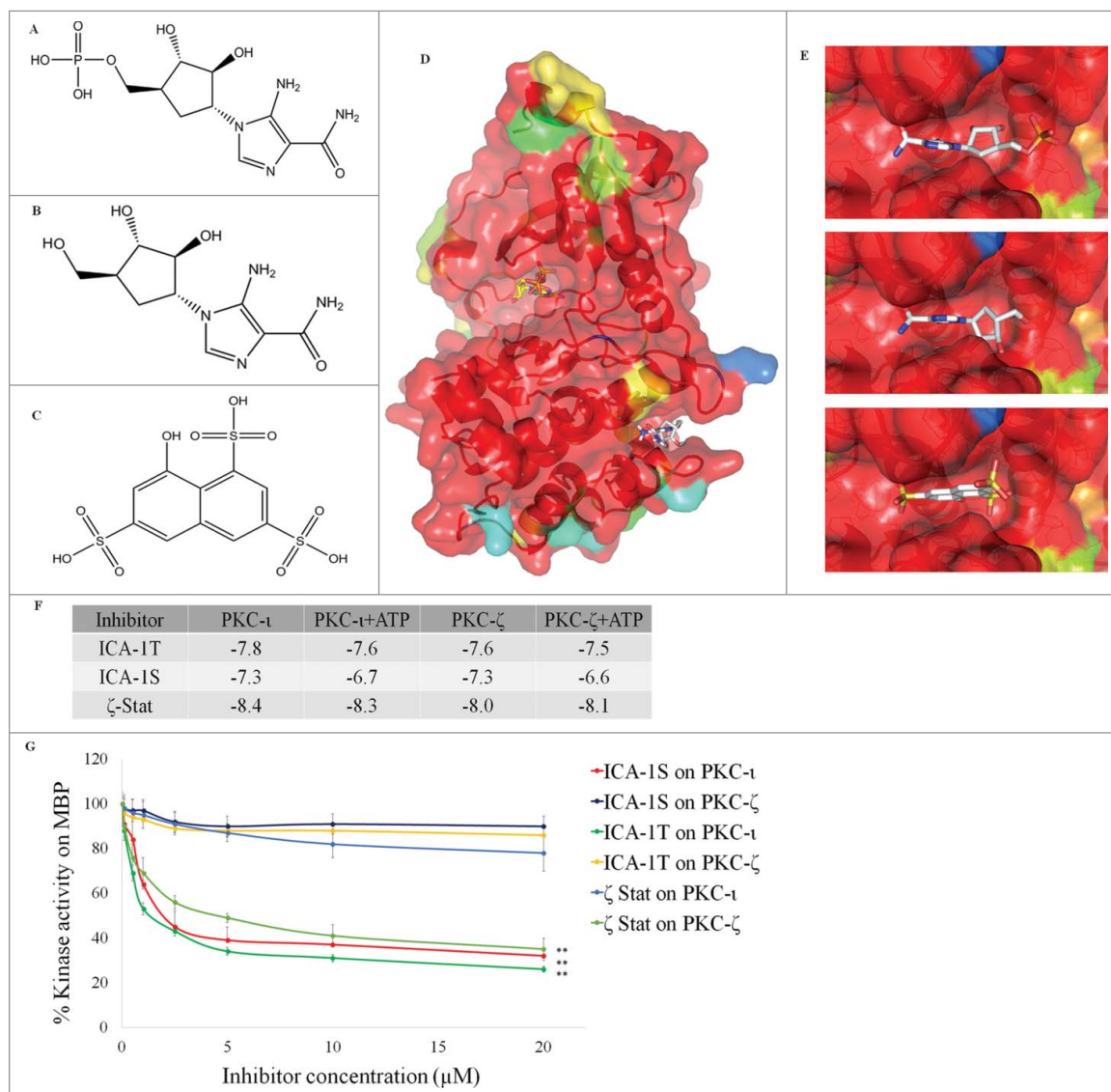


Figure 1. Inhibitor structures, molecular docking and kinase activity. Fig. 1A, 1B and 1C represent molecular structures of ICA-1T (MW = 336.24 g/mol), ICA-1S (MW = 256.26 g/mol) and ζ -Stat (MW = 384.34 g/mol), respectively. Fig. 1D shows the molecular surface of PKC- ι bound to ATP (3A8W) with docked ICA-1T. The molecular surface of residues that differ between PKC- ι and PKC- ζ are colored based on sequence similarity (using the Blosom62 scoring matrix). Blosom62 similarity values are: blue, 40–50, cyan, 50–60, green, 60–70, yellow, 70–90, orange and 90–100, red. Residues that are identical between PKC- ι and PKC- ζ are colored red. ATP is depicted as sticks with yellow for carbon, red for oxygen, blue for nitrogen. ICA-1T is depicted as sticks colored by element with white, red, and blue representing carbon, oxygen, and nitrogen respectively. Fig. 1E shows 3 enlarged pictures of lowest energy docking conformations of ICA-1T, ICA-1S, and ζ -Stat docked in the identified allosteric docking sites. Table in Fig. 1F is a summary of molecular docking scores (ΔG°) in kcal/mol for 3 inhibitors against PKC- ι and PKC- ζ with and without ATP. Fig. 1G represent the effect of ICA-1T, ICA-1S and ζ -Stat on PKC- ι and PKC- ζ activity. Recombinant active PKC- ζ or PKC- ι were incubated with MBP in the presence or absence of inhibitors (0.1– 20 μ M) and percentage kinase activity was plotted against inhibitor concentration. $N = 3$ experiments were performed for each experiment and mean \pm SD are plotted. Statistical significance is indicated by asterisks as $**P < 0.01$.

predictions even though it used a homology model for PKC- ζ . We conducted kinase activity assay (*in-vitro*) of ICA-1S, ICA-1T and ζ -Stat to confirm our virtual screening data. Kinase activities of inhibitors (Figure 1G) were determined for a series of concentrations (0.1– 20 μ M) using recombinant active PKC- ι or PKC- ζ in the presence of MBP. The findings supports virtual screening data obtained for all three compounds.

Both ICA-1S and ICA-1T showed a significant inhibition on PKC- ι ($>60\%$ ($P \leq 0.05$)) but resulting only $\sim 10\%$ inhibition on PKC- ζ . ζ -Stat showed only 13% inhibition on PKC- ι at 20 μ M, but showed a significant inhibition on PKC- ζ as 51% ($P \leq 0.05$) at 5 μ M level. This confirms the specificities we found for ICA-1T and ICA-1S on PKC- ι and the ζ -Stat specificity on PKC- ζ through virtual screening.

Inhibitor dose response curves show significant effects on malignant cell lines

We generated dose curves for inhibitors to investigate effects on cell proliferation of normal and malignant cell lines over a wide range of concentrations. ICA-1T showed no significant effect on MEL-F-NEO (Figure 2A) until up to 5 μ M, but it showed maximum inhibition as 22% ($P \leq 0.05$) at 10 μ M. Both ICA-1S and ζ -Stat showed significant inhibitions on MEL-F-NEO cells beyond 7.5 μ M ($P \leq$

0.05) as 37.7% ($P \leq 0.05$) and 19.3% ($P \leq 0.05$) at 10 μ M, respectively. All inhibitors significantly decreased cell proliferation of SK-MEL-2 and MeWo upon increasing the concentrations. ICA-1T decreased proliferation by 53.1% for 1 μ M ($P \leq 0.01$) in SK-MEL-2 cells (Figure 2B) while 56.1% for 1 μ M ($P \leq 0.01$) in MeWo cells (Figure 2C). ICA-1S decreased proliferation by 46% for 2.5 μ M ($P \leq 0.01$) in SK-MEL-2 cells (Figure 2B) and 50.7% for 2.5 μ M ($P \leq 0.01$) for MeWo cells (Figure 2C). ζ -Stat decreased proliferation by 47.7% for 5 μ M ($P \leq 0.01$) in SK-MEL-2

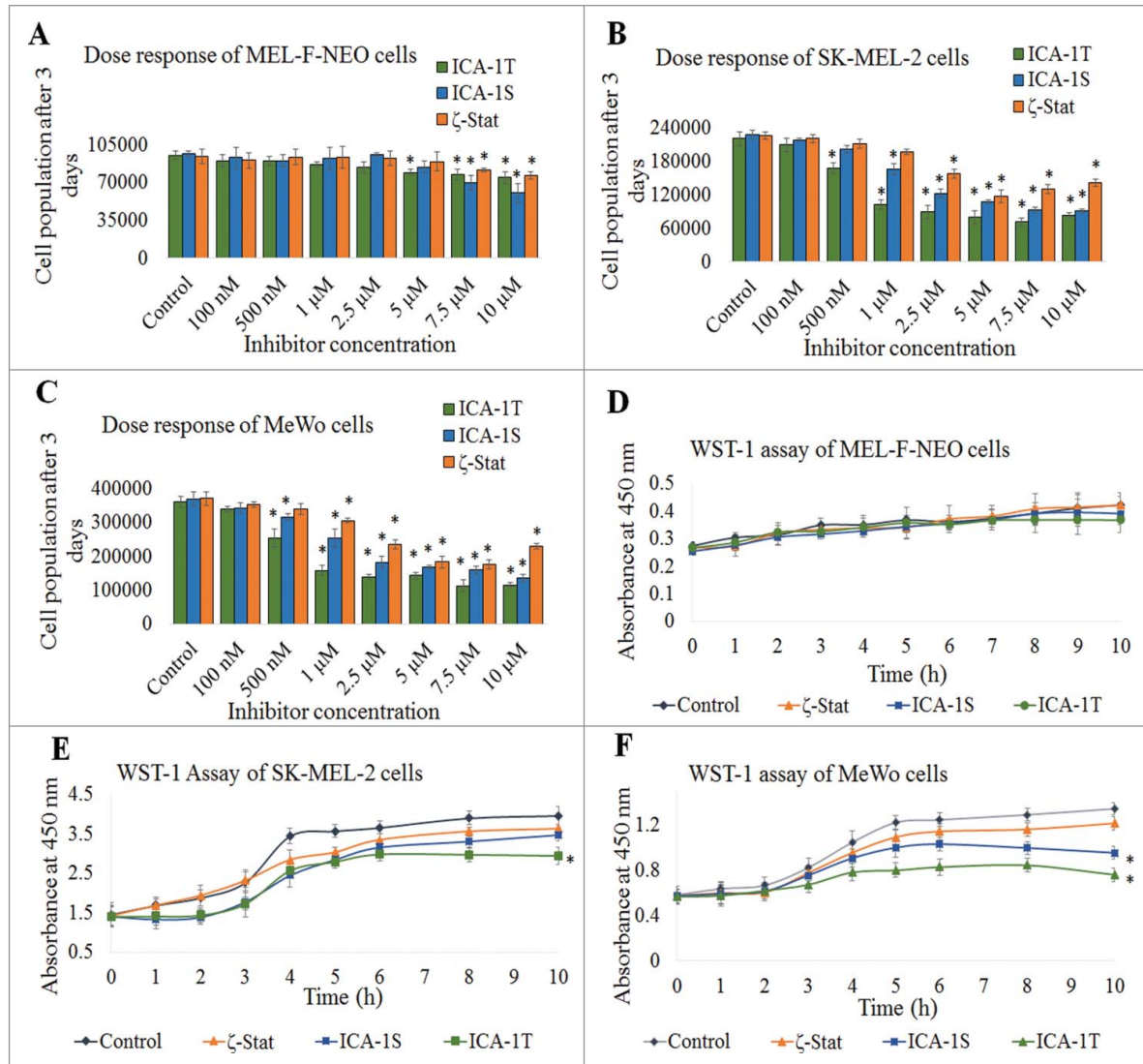


Figure 2. The effects of aPKC inhibitors (ICA-1T, ICA-1S and ζ -stat) on cell proliferation, cell viability and cytotoxicity for melanoma and normal melanocyte cells. Results depict the effect of inhibitors on MEL-F-NEO (Fig. 2A), SK-MEL-2 (Fig. 2B) and MeWo (Fig. 2C) cell proliferation based on cell proliferation assay. Approximately 4×10^4 were cultured in T25 flasks and treated with either equal volume of sterile water (control) or inhibitors (0.1–10 μ M). Additional doses of sterile water or inhibitors were supplied every 24 h during a 3 day incubation period. Subsequently, cells were lifted and counted. Cytotoxicity of aPKC inhibitors was measured using WST-1 assay for MEL-F-NEO (Fig. 2D), SK-MEL-2 (Fig. 2E) and MeWo (Fig. 2F) cells. The absorbance at 450 nm is due to production of water soluble formazan and was measured as a function of time. The absorbance is directly proportional to the number of cells. Experimental concentrations in WST-1 assay for ICA-1T, ICA-1S and ζ -Stat were 1 μ M, 2.5 μ M and 5 μ M, respectively for all three cell lines. The absorbance at 450 nm against time is plotted. Experiments ($N = 3$) were performed for each cell line and mean \pm SD are plotted. Statistical significance is indicated by asterisk as * $P < 0.05$ and ** $P < 0.01$.

cells (Figure 2B) and by 50.6% for 5 μ M ($P \leq 0.01$) for MeWo cells (Figure 2C). Such results suggest inhibitors can effectively decrease cell population without a significant effect on normal melanocytes at the IC_{50} values obtained for inhibitors. IC_{50} values of ICA-1T, ICA-1S and ζ -Stat were found as approximately 1 μ M, 2.5 μ M and 5 μ M, respectively for both cell lines. Later, we used these concentrations in experiments as the testing concentrations.

WST-1 assay for cell viability and cytotoxicity shows inhibitors are cytostatic

To determine the *in-vitro* cytotoxicity of ICA-1T, ICA-1S and ζ -Stat on normal and malignant cell lines, we performed a WST-1 assay. The measured absorbance at 450 nm is directly proportional to the number of viable cells present which produce a water-soluble formazan with WST-1 as a result of their mitochondrial dehydrogenase activity. None of the inhibitors showed significant cytotoxicity on normal melanocytes (Figure 2D). ICA-1T showed a significant cytotoxicity ($P \leq 0.05$) on both melanoma cells followed by ICA-1S. ζ -Stat did not show significant cytotoxicity on both cell lines (Figures 2E and 2F). Results indicate that inhibitors appeared cytostatic more than being cytotoxic during the tested time range, thereby retarding melanoma cell growth and proliferation.

Wound healing assay shows PKC- ι inhibition decreases melanoma cell migration

Wound healing assay was performed to investigate the effect of inhibitors on melanoma cell migration *in-vitro*. Photographs for each cell line were compared as “day 0” (starting point) and “day 3” for both melanoma cell lines (Figure 3A). Moreover, the areas of the scratch (wound) were calculated and compared with respective controls to determine the statistical significance of wound closure for inhibitor treatments (Figure 3B). Compared to 80% wound closure in SK-MEL-2 control, inhibitor treated samples showed fewer wound closures as 28% ($P \leq 0.01$) for ICA-1T at 1 μ M, 33% ($P \leq 0.01$) for ICA-1S at 2.5 μ M and 53% ($P \leq 0.05$) ζ -Stat at 5 μ M. Compared to 66% wound closure in MeWo control, inhibitor treated samples were 26% ($P \leq 0.01$) for ICA-1T at 1 μ M, 32% ($P \leq 0.01$) for ICA-1S at 2.5 μ M and 54% ($P \leq 0.05$) ζ -Stat at 5 μ M. Results suggested ICA-1 is more effective in reducing cell migration *in-vitro* compared to ζ -Stat.

BME invasion assay shows PKC- ι inhibition decreases melanoma cell invasion

BME invasion assay was performed to investigate the effects of ICA-1S, ICA-1T and ζ -Stat on melanoma cell

invasion *in-vitro*. Invaded cells adhered on the bottom surface of transwell inserts were stained with crystal violet and photographs were taken in randomly chosen fields as the visual representation of the invasion assay (Figure 3C). Crystal violet stained invaded cells were dissolved in 70% ethanol in the bottom chamber and absorbance was measured at 590 nm which is proportional to the number of invaded cells (Figure 3D). ICA-1T and ICA-1S significantly ($P \leq 0.01$) reduced invasion by 55% and 43% in SK-MEL-2 cells and by 48% and 44% in MeWo cells, respectively. Interestingly, ζ -Stat did not show a significant effect on decreasing melanoma cell invasion.

Effects of inhibitors on aPKC expression, apoptosis and EMT signaling of melanoma reveal PKC- ι upregulates EMT

We previously reported that PKC- ι and Vimentin were not detected in normal melanocytes compared to higher levels in melanoma cells [6,7]. As shown in Figure 4A, Western blots revealed that both ICA-1T and ICA-1S significantly reduced total and phosphorylated PKC- ι while having no effect on PKC- ζ . ζ -Stat showed a significant diminution of phosphorylated and total PKC- ζ levels. Since all inhibitors significantly reduce melanoma cell proliferation, we tested the potential of the inhibitors on inducing the apoptosis. Caspase-3 and cleaved-PARP levels were significantly increased and Bcl-2 and PARP levels were significantly diminished upon inhibitor treatments. We have also investigated the effects of aPKC inhibition on EMT signaling and how cascades such as Wnt/ β -catenin, NF- κ B, AKT are affected by aPKC inhibition during EMT stimulation. We tested the levels of β -catenin, phosphorylated PTEN (S380), phosphorylated AKT (S473), IKB α and phosphorylated IKB α , phosphorylated IKK α/β (S176/180), NF- κ B p65 in cytoplasm and in nucleus, E-cadherin, phosphorylated Vimentin (S39), Par6 and RhoA. β -catenin levels did not change significantly while phospho PTEN, phospho AKT, phospho IKB α , phospho IKK α/β and nucleic NF- κ B p65 significantly decreased and levels of IKB α and cytoplasmic NF- κ B p65 significantly increased as a result of the three inhibitors.

Inhibition of PKC- ζ using ζ -Stat showed no significant effect on E-cadherin, Vimentin and phospho-Vimentin or Par6 and RhoA. Conversely, ICA-1T and ICA-1S inhibition on PKC- ι resulted in a significant increase of E-cadherin and RhoA while significantly decreasing Vimentin, phospho-Vimentin and Par6.

We have also tested the effects of TNF- α and TGF β stimulation on aPKC expression. As shown in Figure 5A, we found that protein levels and the degree of

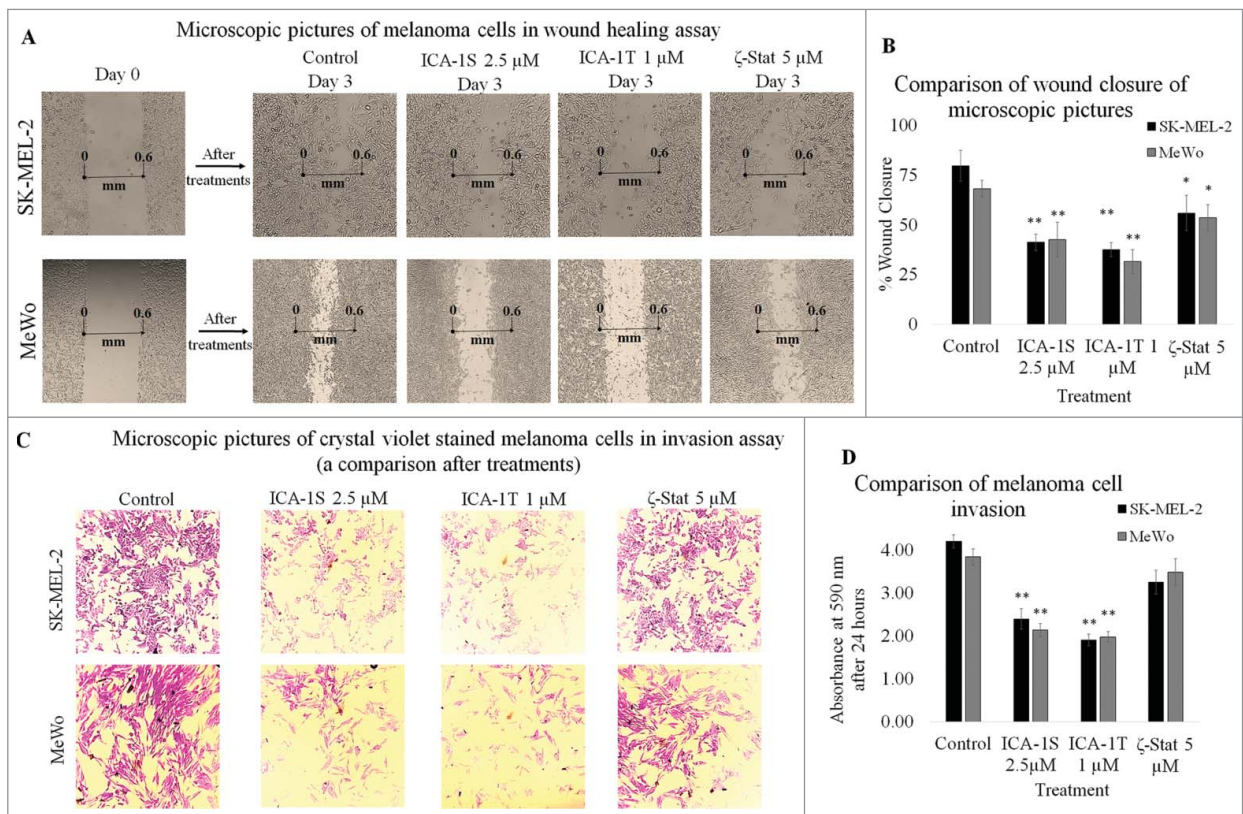


Figure 3. Inhibitors decrease melanoma cell migration and invasion. Fig. 3A and 3B represent the effect of aPKC inhibitors (2.5 μM of ICA-1S, 1 μM of ICA-1T and 5 μM of ζ -Stat) on melanoma cell migration in wound healing assay and Fig. 3C and 3D represent the effect of inhibitors on melanoma cell invasion in Boyden chamber assay with basement extract (BME). In the wound healing assay, microscopic photographs (40 \times) of scratches on cells at the beginning (day 0) were compared with the photographs taken after 3 days. The effect of inhibitors are shown (Fig. 3A) compared to their controls. Experiments ($N = 3$) were performed for each cell line and randomly picked photographs are shown. Fig. 3B represents a comparison of calculated percent wound closure for the photographs taken using ImageJ (NIH, Rockville, MD, USA). For Boyden chamber assay (Fig. 3C), invaded cells in the bottom surface of transwell insert were stained with 0.5% crystal violet and microscopic pictures were taken (100 \times). Subsequently, crystal violet was dissolved in 70% ethanol and absorbance was measured at 590 nm which directly proportional to the number of invaded cells. Mean \pm SD are plotted. Statistical significance is indicated by asterisk as $**P < 0.01$.

phosphorylation significantly increased for both aPKCs in the presence of $\text{TNF-}\alpha$ and $\text{TGF}\beta$, thereby significantly heightening phosphorylation on PTEN (S380), AKT (S473), $\text{IKK}\alpha/\beta$ (S176/180), $\text{IKB}\alpha$ (S32) and Vimentin (S39) which resulted in enhancing Bcl-2, $\text{NF-}\kappa\text{B}$ translocation and degradation of E-cadherin and RhoA. All values (percent) were calculated compared to their respective controls in Western blots (Figure 4B and 5B; densitometry analysis) and significance was indicated as $P \leq 0.05$. β -actin was used as the internal control to ensure equal amounts of proteins were loaded in each lane in the SDS-PAGE.

Immunoprecipitation, immunofluorescence microscopy and qPCR experiments confirm the activation of Vimentin by PKC- ι

We previously suggested that PKC- ι associates with Vimentin, but Vimentin showed no association with

PKC- ζ . Its association with Vimentin was confirmed with immunoprecipitation of PKC- ι and Vimentin [6]. Figure 6A shows that siRNA knockdown of PKC- ι confirmed the association with Vimentin by significantly abating the total Vimentin and phosphorylated Vimentin while increasing E-cadherin. PKC- ζ knockdown showed no effect on those proteins. Interestingly, silencing both PKC- ι and PKC- ζ did show a significant effect on $\text{NF-}\kappa\text{B}$ translocation by diminishing the level of $\text{NF-}\kappa\text{B}$ p65. Previous reports highlighted that both aPKCs associate with Par6 to make aPKC/Par complex [20,21]. Here, we immunoprecipitated Par6 and immunoblotted for both PKC- ι and PKC- ζ as shown in Figure 6B. Immunoblots revealed that only PKC- ι associate with Par6 in both melanoma cell lines. Reverse immunoprecipitation of PKC- ι confirmed the band obtained for Par6, thereby also confirming the association between PKC- ι and Par6 (Figure 6B).

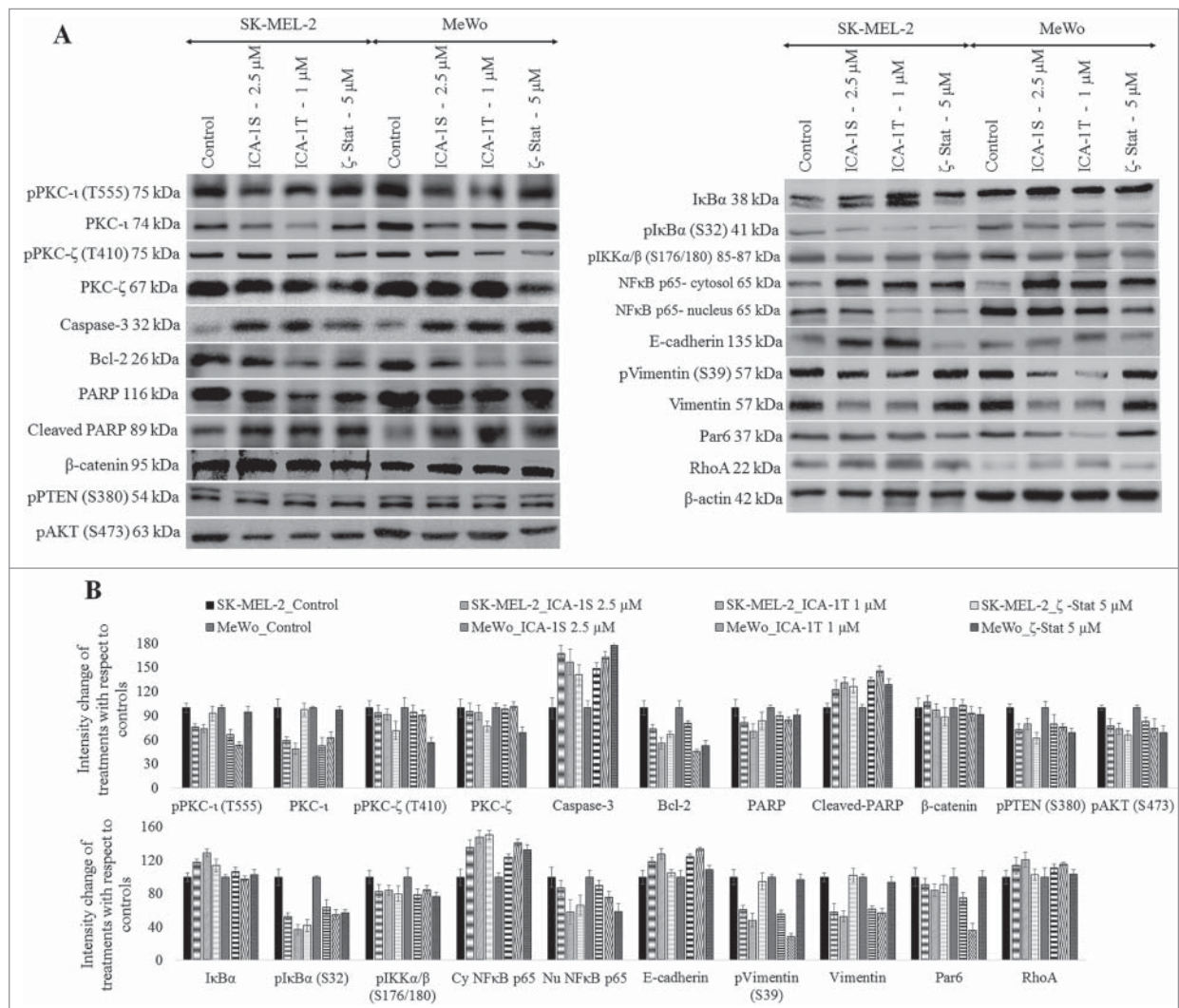


Figure 4. Effect of inhibitors (ICA-1S, ICA-1T and ζ -Stat) on aPKC expression, apoptosis, and signaling pathways related to EMT in melanoma cells. Expression of the protein levels of phosphorylated PKC- ι , total PKC- ι , phosphorylated PKC- ζ , total PKC- ζ , Caspase-3, cleaved PARP, total PARP, Bcl-2, β -catenin, Vimentin, phosphorylated Vimentin, Par6, phosphorylated PTEN, RhoA, E-cadherin, phosphorylated AKT and NF- κ B p65, I κ B, phosphorylated I κ B and phosphorylated IKK α / β for the inhibitor treatments (2.5 μ M of ICA-1S, 1 μ M of ICA-1T and 5 μ M of ζ -Stat) are shown in Fig. 4A. 40–80 μ g of protein was loaded in to each well and β -actin was used as the loading control in each Western blot. Fig. 4B represents the densitometry values for Western blots in Fig. 4A. Experiments ($N = 3$) were performed in each trial and representative bands are shown.

Figure 6C shows that immunofluorescence staining also confirmed the association of PKC- ι and Vimentin depicting both proteins distributed throughout the cytoplasm. ICA-1T treated cells showed lesser of those proteins (lighter in staining) compared to controls. Inhibitor treatments for both cell lines also decreased the nuclei and overall cell sizes. In the controls of both cells, the invasive characteristics such as formation of lamellipodia, filopodia and invadopodia are observable clearly whereas ICA-1T treated cells showed less of such features.

As Figure 7 demonstrates, qPCR data revealed that PKC- ι mRNA levels decreased upon having been treated with ICA-1T and ICA-1S, by approximately 50% in SK-MEL-2 cells and 30% in MeWo cells (Figures 7A and 7E,

respectively). There was no significant difference observed between the inhibition of PKC- ι by ICA-1T and ICA-1S. Vimentin mRNA levels decreased by approximately 50% in SK-MEL-2 cells (Figure 7C) when treated with either PKC- ι inhibitor. Vimentin mRNA levels had no significant changes in MeWo cells treated with either ICA-1T or ICA-1S (Figure 7G). ζ -Stat treatments had no significant effect on Vimentin mRNA levels in either cell line.

Discussion

We were able to confirm the presence of a potentially druggable allosteric site in the structure of PKC- ι using solved crystal structure of PKC- ι . This site was identified

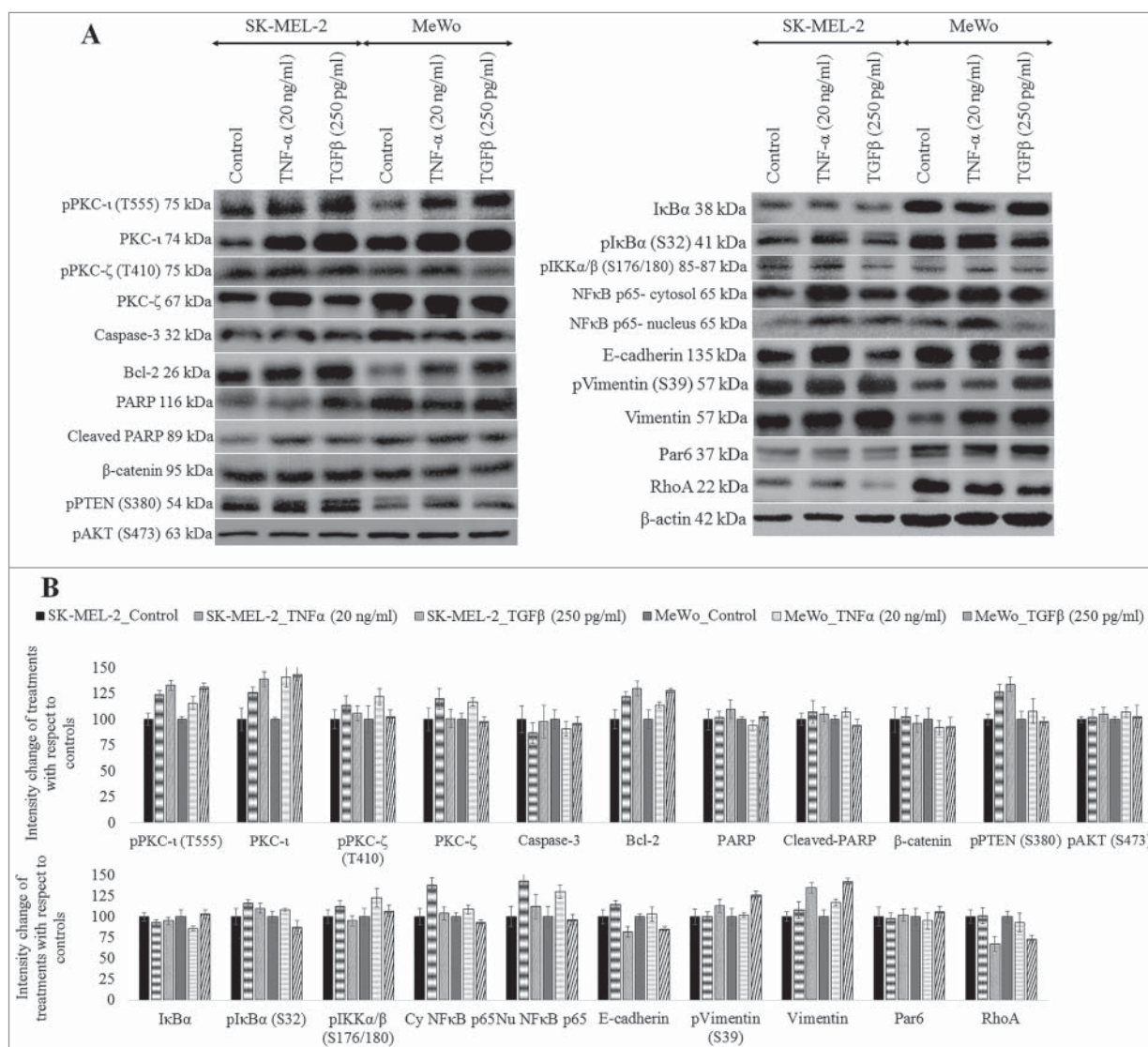


Figure 5. Effect of TNF- α and TGF β on aPKC expression, apoptosis, and signaling pathways related to EMT in melanoma cells. Expression of the protein levels of phosphorylated PKC- ι , total PKC- ι , phosphorylated PKC- ζ , total PKC- ζ , Caspase-3, cleaved PARP, total PARP, Bcl-2, β -catenin, Vimentin, phosphorylated Vimentin, Par6, phosphorylated PTEN, RhoA, E-cadherin, phosphorylated AKT and NF- κ B p65, I κ B, phosphorylated I κ B and phosphorylated IKK α/β for the TNF- α (20 ng/ml) and TGF β (250 pg/ml) treatments are shown in Fig. 5A for malignant melanoma cell lines (SK-MEL-2 and MeWo) are shown after the end of third day of treatments with respect to their controls. 40–80 μ g of protein was loaded in to each well and β -actin was used as the loading control in each Western blot. Fig. 5B represents the densitometry values for Western blots in Fig. 5A. Experiments ($N = 3$) were performed in each trial and representative bands are shown.

using a PKC- ι homology model by Pillai, *et al* [11]. This site, within the C-lobe of the kinase domain, is framed by solvent exposed residues of helices α F- α I and the activation segment. PKC- ι inhibitors were predicted to interact with this site with moderate affinity based on molecular docking. Combinations of drugs targeting the ATP binding site and allosteric sites would be expected to more effectively inhibit cancer cell growth.

It was essential to determine the cytotoxicity of the inhibitors to establish the therapeutic potential of the inhibitors. All three inhibitors were non-toxic to normal melanocytes, and showed an insignificant effect on

proliferation and viability at the IC₅₀ used for two melanoma cell lines. On the other hand, the three inhibitors showed more cytostatic properties on melanoma cells with a mild toxicity provided by ICA-1T and ICA-1S at their IC₅₀ values. The results show that inhibitors are effective in arresting malignant melanoma cells in terms of their growth, differentiation and proliferation before they induce apoptosis. This confirms that malignant melanoma cells are highly dependent on aPKCs to remain viable, supporting our previous data that both melanoma cell lines overexpress aPKCs compared to the undetectable PKC- ι and low levels of PKC- ζ in MEL-F-NEO cells [6].

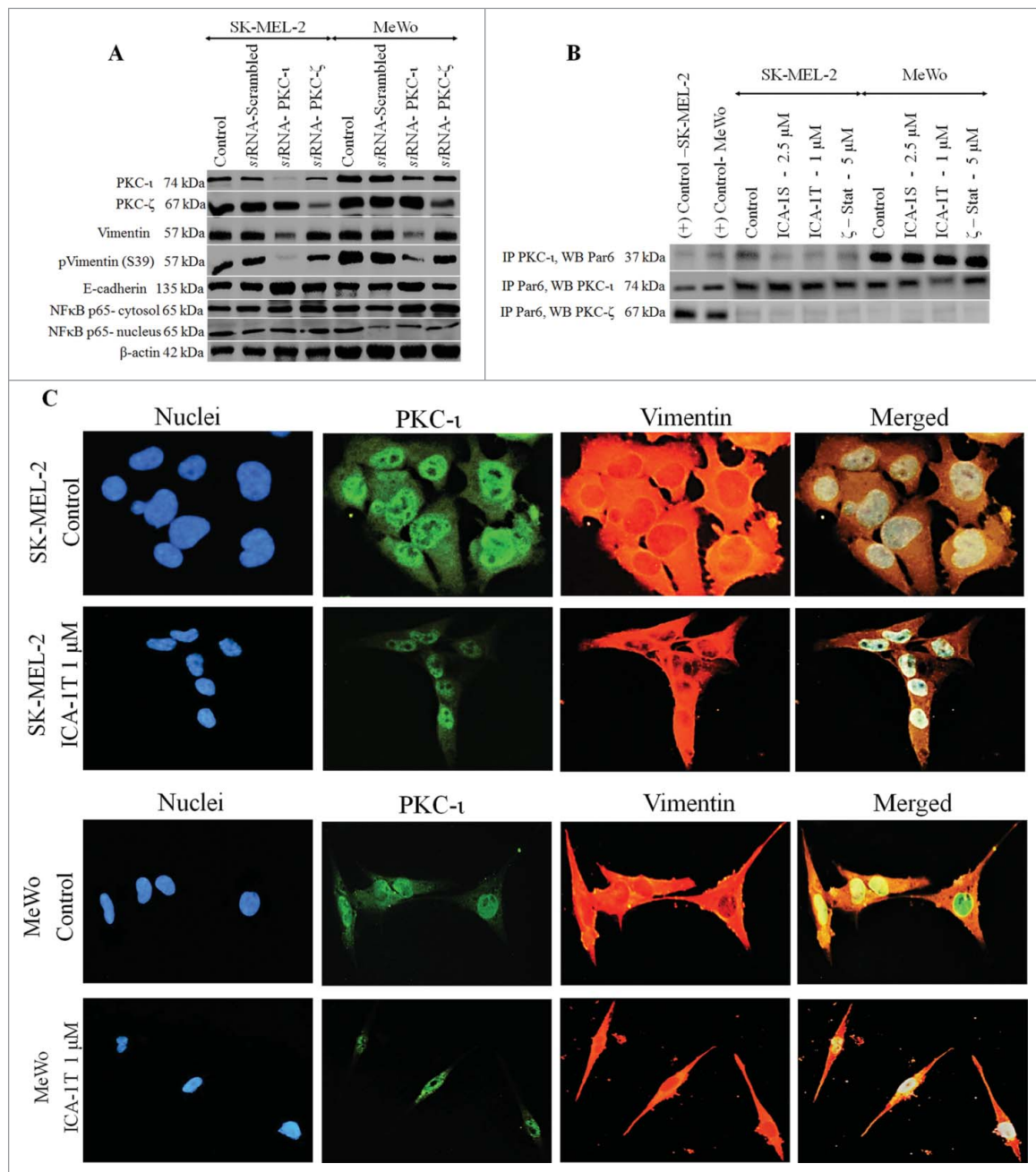


Figure 6. PKC- ι activates Vimentin and both aPKCs stimulate nuclei translocation of NF- κ B in melanoma cells. The effects of on siRNA knockdown (20 nM of PKC- ι and PKC- ζ siRNA) on the expression of aPKCs, Vimentin activation and NF- κ B translocation are shown in Fig. 6A. 40 μ g of protein was loaded in to each well and β -actin was used as the loading control in each Western blot. Fig. 6B is shown the association between PKC- ι and Par6. Whole cell lysates (100 μ g) of malignant cells (Sk-Mel-2 and MeWo) were immunoprecipitated separately for PKC- ι and Par6 using specific antibodies. First two lanes in Western blot represents the (+) control which contained 40 μ g of Sk-MEL-2 and MeWo whole cell extracts, respectively, applied to ensure that bands appeared for the specific proteins in Western blots. Western blots of PKC- ι immunoprecipitation showed an association with Par6. Reverse-immunoprecipitation of Par6 confirmed the association with PKC- ι while no association was observed with PKC- ζ . Fig. 6C represents the immunofluorescence staining of nuclei (blue panel), PKC- ι (green panel) and Vimentin (red panel) for melanoma cells (SK-MEL-2 and MeWo) treated with ICA-1T (1 μ M) against controls. The images were captured at 200X magnification. Experiments ($N = 3$) were performed in each trial.

Overexpression of aPKCs is often associated with anti-apoptotic effects in many cancers. Reduction in the total protein levels, as well as the phosphorylated levels, were observed for PKC- ι in ICA-1T and ICA-1S

treatments whereas for PKC- ζ in ζ -Stat treatments. An increase in Caspase-3 and PARP cleavage, and a decrease in Bcl-2 all indicate apoptosis stimulation upon inhibition of both PKC- ι and PKC- ζ (Figures 4A and 4B). One

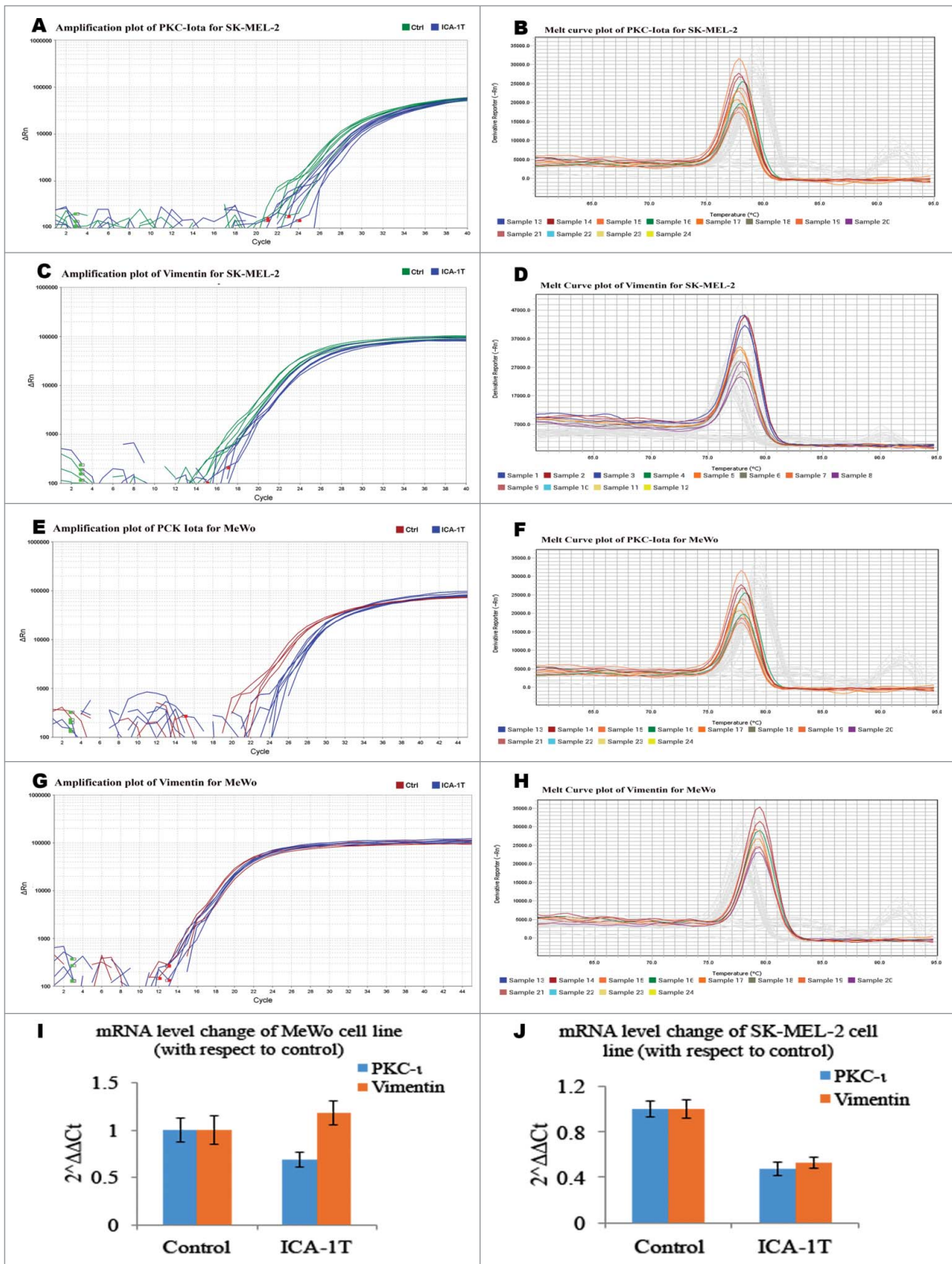


Figure 7. Quantitative real time PCR data of ICA-1T (1μ M) treatments for PKC- ι and Vimentin for melanoma cell lines. Fig. 7A and 7C represent the amplification plots of PKC- ι and Vimentin for SK-MEL-2 cell line. Fig. 7E and 7G represent the amplification plots of PKC- ι and Vimentin for MeWo cell line. Fig. 7B and 7D represent the melt curve plots of PKC- ι and Vimentin for SK-MEL-2 cell line. Fig. 7F and 7H represent the melt curve plots of PKC- ι and Vimentin for SK-MEL-2 cell line. Fig. 7I and 7J demonstrate the mRNA level change of PKC- ι and Vimentin for ICA-1T treated MeWo and SK-MEL-2 cell lines, respectively. The $\Delta\Delta Ct$ values were plotted with respect to the mRNA levels of control samples of each cell line. Statistical significance is indicated by asterisk as $*P < 0.05$. Experiments ($N = 3$) were performed in each trial.

major anti-apoptotic pathway is PI3K/AKT mediated NF- κ B activation, wherein aPKCs play a role in releasing NF- κ B to translocate to the nucleus and promote cell survival. PI3K stimulates IKK α/β through activation of AKT by phosphorylation at S473, which ultimately stimulates translocation of NF- κ B complex into the nucleus, boosting cell survival [22]. PTEN regulates the levels of PI3K. Phosphorylation at S380 leads to the inactivation of PTEN, thereby increasing the levels of PI3K followed by enhancement in phospho-AKT. Inhibition of PKC- ι and PKC- ζ significantly decreased the levels of phospho-PTEN and phospho-AKT but we still found increases in NF- κ B p65 levels in the cytosol after inhibiting both aPKCs. This may seem illogical, but previous studies have shown that expression of NF- κ B p65 has a corresponding increase in I κ B, resulting in an auto-regulatory loop [22]. Moreover, negative feedback is not inhibiting upstream signaling for NF- κ B translocation because translocation has been inhibited downstream, resulting in more NF- κ B production. Knowing this, we tested the levels of NF- κ B translocation by separating the nuclear extracts from the cell lysates and found that NF- κ B levels in the nuclei decreased upon aPKC inhibition. This suggested that translocation of activated NF- κ B in to nuclei is inhibited as a result of inhibition of aPKCs. We also found that aPKC inhibition increased the levels of I κ B while decreasing the levels of phospho-I κ B (S32) and phospho-IKK α/β (S176/180), confirming that both PKC- ι and PKC- ζ play a role in phosphorylation of IKK α/β and I κ B: increased levels of I κ B therefore remain bound to NF- κ B complex and prevent the translocation to the nucleus to promote cell survival (Figure 8). We also tested the effects of TNF- α stimulation on the expression of aPKCs (Figures 5A and 5B). TNF- α is a cytokine, involved in the early phase of acute inflammation by activating NF- κ B. TNF- α stimulation significantly increased NF- κ B levels in both cytosol and nuclei. Increased NF- κ B production promotes increases in total and phosphorylated aPKCs and increased Bcl-2 levels, which enhances melanoma cell survival. We observed heightened levels of I κ B and NF- κ B, which together enhance the phosphorylation of I κ B because of the augmented aPKCs. This confirms that both PKC- ζ and PKC- ι are embedded in cellular survival via NF- κ B and PI3K/AKT pathways.

During EMT, epithelial cells lose apical-basal polarity, remodel the extra cellular matrix (ECM), rearrange the cytoskeleton, undergo changes in signaling programs that control the cell shape maintenance and alter gene expression to acquire mesenchymal phenotype, which is invasive and increases individual cell motility [23]. EMT's key features include downregulation of epithelial genes such as E-cadherin to destabilize tight junctions

between cells and upregulation of genes that assist mesenchymal phenotype such as Vimentin. Before testing protein levels in Western blots, we tested the effects of inhibitors on melanoma cell migration and invasion (Figure 3). Migration and invasion studies in cancer research are very important because the main cause of death in cancer patients is related to metastatic progression. For cancer cells to spread and disseminate throughout the body, they must migrate and invade through ECM, intravasate into blood stream and extravasate to form distant tumors [24]. Both migration and invasion were markedly reduced for the samples treated with ICA-1T and ICA-1S compared to ζ -Stat treated samples, suggesting that PKC- ι inhibition significantly slows down melanoma cell migration and invasion. This suggests that PKC- ι is involved in EMT in melanoma. It has been previously shown that aPKC/Par6 signaling stimulates EMT upon activation of TGF- β receptors. RhoA is a GTPase, which promotes actin stress fiber formation thereby maintains cell integrity. TGF- β activation stimulates degradation of RhoA which leads to the depolymerization of filamentous actin (F-actin) and loss of structural integrity resulting a reduction in cell-cell adhesion [20]. Furthermore, TGF β upregulates SNAIL, a transcription factor that upregulates EMT through the Smad signaling pathway [25]. Cells lose E-cadherin while gaining Vimentin during this process. As shown in Figure 4A, inhibition of PKC- ι using ICA-1T and ICA-1S significantly increased the levels of E-cadherin and RhoA while decreasing total and phospho-Vimentin (S39) and Par6. None of those protein levels were significantly changed as a result of PKC- ζ inhibition. We also tested the effects of TGF β stimulation on the markers that we tested for the aPKC inhibition. TGF β increased the levels of PKC- ι , Vimentin, phospho-Vimentin and Par6 while decreasing E-cadherin and RhoA. This confirmed the involvement of PKC- ι in EMT stimulation.

Immunoprecipitation of PKC- ι showed a strong association with Par6 in both melanoma cells which was confirmed with reverse-immunoprecipitation of Par6 (Figure 6B). Previously published reports state that both aPKCs associate with Par6 and phosphorylate at S345 [21,26]. In the present study, only PKC- ι showed an association with Par6, which confirmed that PKC- ι is a major activator of EMT in melanoma. In addition, we previously showed that PKC- ι strongly associates with Vimentin [6].

siRNA knockdown of PKC- ι and PKC- ζ , immunofluorescent staining and qPCR results confirmed the association of Vimentin. As we demonstrate in Figure 6A, silencing PKC- ι significantly decreased the total and Phospho-Vimentin and increased the E-cadherin. This further confirms the results observed upon

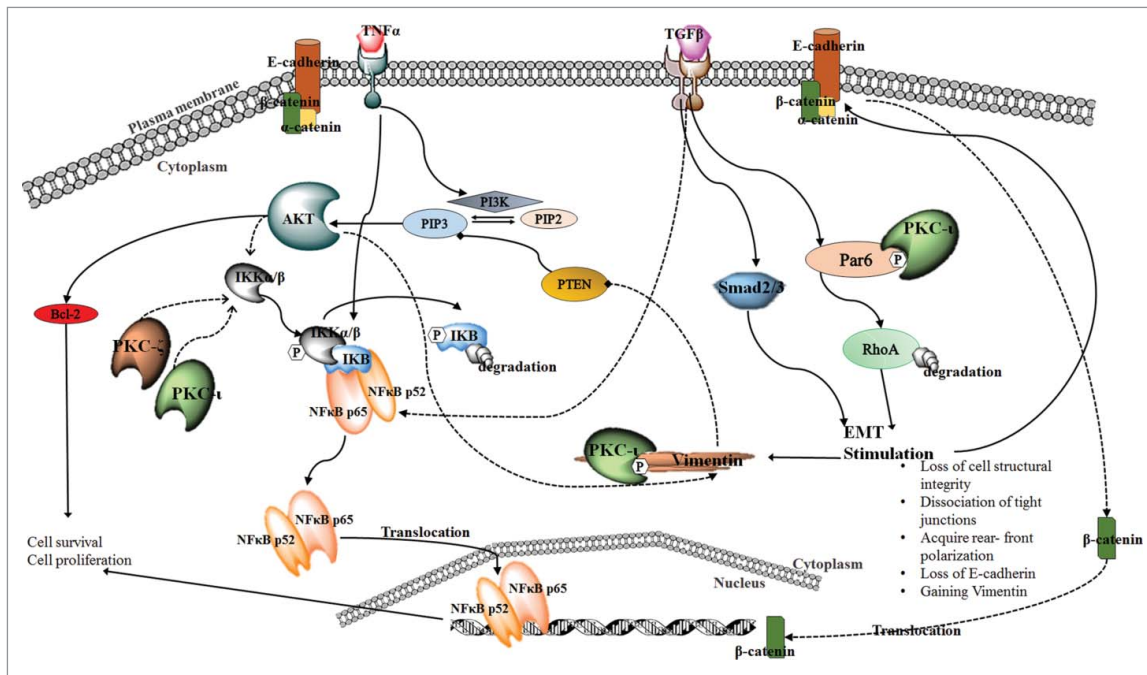


Figure 8. A schematic summary of the involvement of PKC- ι and PKC- ζ in melanoma progression. Upon extra cellular stimulation with TNF- α and TGF β , PKC- ι activates Par6, which leads to the degradation of RhoA and stimulates EMT by changing the cell integrity, loss of E-cadherin and gain of Vimentin. During this process, cadherin junctions will be destabilized as a result of loss of E-cadherin and β -catenin will be translocated to nucleus to upregulate the production of some proteins such as CD44 which further stimulate migration and EMT. Importantly PKC- ι tightly binds to Vimentin to activate them by phosphorylation and this activated Vimentin changes the cell polarity to maintain the mesenchymal phenotype. Activated Vimentin can also induce the phosphorylation of PTEN leading to inactivation of inhibitory action of PTEN on PIP3 [40]. This may result in activation of AKT through PIP3 and activated AKT pathway leading to cell survival, rapid proliferation and differentiation which are critical parts of melanoma progression. AKT could indirectly stimulate β -catenin translocation and activate NF- κ B pathway in which PKC- ζ is known to play a stimulatory role on IKK- α/β . It is reported that activated NF- κ B can inhibit PTEN [35].

specific inhibition of aPKCs. Moreover, it confirmed that both aPKCs regulate the translocation of NF- κ B to the nucleus showing a decrease in nuclei NF- κ B levels. Figure 6C exhibits how immunofluorescence staining revealed that the shape of melanoma cells significantly changed upon inhibition of PKC- ι . Both Vimentin and PKC- ι levels were relatively low in ICA-1T treated cells in comparison to their respective controls. In addition to that, invasive characteristics such as formation of lamellipodia, filopodia and invadopodia were distinctively visible in both controls, though they were not apparent in treated cells. This also confirmed the growth retardation we observed in melanoma cells upon aPKC inhibitor treatments that had resulted in lesser growth in treated cells. As observed in qPCR experiments, treatments with PKC- ι specific ICA-1T and ICA-1S, thereby the corresponding downregulation of PKC- ι suggested that PKC- ι plays a role in its own regulation. Phosphorylation of Vimentin at S39 is required for its activation and inhibition of PKC- ι diminishes this activation process. Very low levels of total Vimentin observed in Western blots for ICA-1T and ICA-1S treated cells indicate that without PKC- ι ,

unphosphorylated Vimentin undergoes rapid degradation. In addition to activating Vimentin, PKC- ι appears to play a role in regulating Vimentin expression in some carcinoma cells [27,28].

Western blots of β -catenin did not show significant change in its levels upon aPKC inhibition (Figure 4A) and TNF- α or TGF- β stimulations (Figure 5A). This could be due to its stabilization by preventing its degradation even after dissociation from the cadherin junctions, for the purpose of transcription in the Wnt signaling pathway [29]. α 1 β 1 or α 2 β 1 integrins usually facilitate this translocation by disrupting the E-cadherin complexes thereby promoting nuclei translocation of β -catenin [30]. Translocated β -catenin continuously drives transcription of targeted genes such as CD44. CD44 is a transmembrane glycoprotein upregulated by Wnt5A, and act as an important mediator in tumor progression and cell invasion [31]. PI3K-AKT, NF- κ B and WNT signaling pathways indirectly promote EMT by stabilizing SNAIL1 through disruption of GSK3 β -SNAIL1 interactions [32-34]. Activated Vimentin can inhibit PTEN by increasing the phosphorylation of PTEN to enhance PI3K/AKT activity, causing cell

differentiation and survival of osteoblasts [35]. Just as summarized in Figure 8, inhibition of aPKCs in melanoma (with emphasis to PKC- ι) can therefore suppress tumorigenesis by retarding growth, differentiation, survival and invasion of cells *in-vitro*.

In conclusion, the results in the present study suggest that PKC- ι is major component responsible for inducing cell growth, differentiation, survival and EMT, while PKC- ζ is mainly involved in NF- κ B signaling to promote cell growth and survival in human melanoma cells *in-vitro*. In addition, PKC- ι is involved in activation of Vimentin thereby driving major cytoskeletal changes essential for EMT. Our results also suggest that ICA-1T, ICA-1S and ζ -Stat are effective aPKC inhibitors in melanoma cells and do not affect normal melanocytes at the best working concentrations for melanoma cells *in-vitro*. These inhibitors can reduce the cell proliferation, migration and invasion, while inducing apoptosis. The inhibitors should be further tested *in-vivo* to determine their therapeutic potentials. Results also confirmed the direct relationship between Vimentin, PKC- ι and EMT. PKC- ι inhibition can reduce EMT progression, or even possibly reverse it by specifically inhibiting PKC- ι . Finally, the evidence we collected indicates PKC- ι and PKC- ζ are potential therapeutic targets for metastatic melanoma.

Materials and methods

Materials

ICA-1 nucleotide (ICA-1T) and nucleoside (ICA-1S) were synthesized by Therachem (Jaipur, India) and ζ -Stat was obtained from the National Institute of Health (NIH) (Bethesda, MD, USA). They were dissolved in sterile distilled water (vehicle) before use. Antibodies were purchased as follows. PKC- ι (610175) and Bcl-2 (610538) from BD Biosciences (San Jose, CA, USA), PKC- ζ (sc-17781), NF- κ B p65 (sc-372-G), IKB α (sc-1643), Phospho IKB α (sc-8404) and Caspase-3 (sc-7272) from Santa Cruz Biotech (Santa Cruz, CA, USA), phospho PKC- ζ (T410) (PA5-17837), Phospho PKC- ι (T555) (44-968G), E-Cadherin (701134), Vimentin (MA3-745) and Myelin basic protein (MBP) (PA1-10008) from Thermo Fisher Scientific (Waltham, MA, USA), phospho Vimentin (S39) (13614S), phospho PTEN (S380) (9551), phospho AKT (S473) (4059S), phospho IKK α/β (S176/180) (2697), PARP (9532) and cleaved-PARP (9185) from Cell Signaling (Danvers, MA, USA). β -actin-peroxidase (A3854) from Sigma (St. Louis, MO, USA). RhoA (ab54835) and β -catenin (ab16051) from Abcam (Cambridge, MA, USA). Phospho MBP (T125) (05-429) from EMD Millipore (Billerica, MA, USA). Enhanced chemiluminescence

solution (34080) was purchased from Pierce (Rockford, IL, USA). Dulbecco's phosphate buffered saline without Mg²⁺ and Ca²⁺ (D8537) and Trypsin-EDTA (Ethylene-diaminetetraacetic acid) solution (T4049) were purchased from Sigma Aldrich. 4-[3-(4-iodophenyl)-2-(4-nitrophenyl)]-2H-5-tetrazolio]-1,3-benzene disulfonate (WST-1) reagent for cell proliferation (11644807001) was purchased from Roche Diagnostics (Mannheim, Germany). Basement membrane extraction (BME) (3455-096-02) was purchased from Trevigen (Gaithersburg, MD, USA). Human recombinant proteins PKC- ι (PV3183), PKC- ζ (P2273), TNF α (10602HNAE25), TGF β 1 (PHG9204) and MBP (MBS717422) were purchased from Thermo Fisher (Waltham, MA, USA) and MyBioSource (San Diego, CA, USA) respectively. Human small interfering RNA (siRNA) for PKC- ι (SR303741) and for PKC- ζ (303747) were purchased from OriGene (Rockville, MD, USA).

Molecular docking

ICA-1T, ICA-1S, and ζ -Stat were docked on solved crystal structures of PKC- ι with and without bound ATP (PDB 3A8W, 3A8X) using the molecular docking program AutoDock Vina [36]. The three dimensional compound structures were translated from SMILES string to PDB file using the NCI/CADD translator (<https://cactus.nci.nih.gov/translate/>) [37]. SWISS-MODELS of PKC- ζ were generated using the human PKC- ζ sequence (UniProt Q05513) and the crystallized PKC- ι structures as templates. Modeled PKC- ζ structures were processed for geometric minimization using Phenix (v 1.11.1-2575). Ligands and PKC structures were prepared for docking using AutoDockTools 1.5.6 (9_17_14 build). Molecular docking was performed using AutoDock Vina 1.1.2 (May 11, 2011 build). Top scoring docked ligand conformations, ranked by lowest kcal/mol scores coupled with visual inspections, were then selected for localized Vina screening. Docking output files were visualized with, and molecular images generated using Pymol (v 1.7.2.1). All molecular docking tasks were performed on a high performance workstation running Linux.

Cell culture

SK-MEL-2 (ATCC[®] HTB-68TM) and MeWo (ATCC[®] HTB-65TM) cell lines were purchased from American Type Tissue Culture Collection (ATTC; Rockville, MD, USA) in November, 2015 and MEL-F-NEO cell line was purchased from Zen-Bio, Inc. (Research Triangle Park, NC, USA) in December, 2016. All cells were frozen in liquid nitrogen immediately with early passages. The cells of passages 2 to 5 were resuscitated from liquid nitrogen stocks and cultured for less than 3

months before re-initiating culture from the same passage for each tested experiment. Both ATCC and Zen-Bio, Inc. had authenticated the cell lines using morphology, karyotyping and PCR-based approaches. Cells were cultured at 37°C and 5% CO₂.

Melanocyte growth medium (MEL-2) was used for MEL-F-NEO cell culturing according to the instruction manual. Eagle's minimum essential media (90% v/v) (ATCC 30–2003) with fetal bovine serum (10% v/v) and Penicillin (5 µg/ml) were used for SK-MEL-2 and MeWo cell culturing according to ATTC guidelines. All cell lines were seeded and grown as monolayers in T25 or T75 flasks.

PKC activity assay

PKC activity assay was conducted by monitoring the phosphorylation of MBP (0.025 mg/ml), a known substrate for PKCs. The detailed procedure was performed as described in Pillai, et al. for ICA-1S, ICA-1T and ζ-Stat (0.1–20 µM) on recombinant PKC-ι and PKC-ζ (0.01 µg/µl)¹¹. Samples then fractionated by SDS-PAGE and immunoblotted for phosphorylated MBP. Kinase activity was calculated based on the densitometry values of Western blots.

Inhibitor dose response curves and WST-1 assay for cell viability and cytotoxicity

MEL-F-NEO, SK-MEL-2 and MeWo cells (4×10^4) were cultured in T25 flasks and treated with either an equal volume of sterile water (vehicle control) or inhibitors (ICA-1S, ICA-1T and ζ-Stat) using a series of concentrations (0.1–10 µM). The detailed procedure was performed as described in Ratnayake, et al [6].

WST-1 assay was performed culturing approximately 4×10^3 cells/well (MEL-F-NEO, SK-MEL-2 and MeWo) in a 96 well plate. After 24 h post plating time, fresh media were supplied (200 µl/well) and treated with either an equal volume of sterile water (vehicle control) or with the IC₅₀ concentrations of ICA-1T (1 µM) or ICA-1S (2.5 µM) or ζ-Stat (5 µM). These IC₅₀ values were obtained based on the dose response curves. The detailed procedure was performed as described in Ratnayake, et al [6].

Assays for cell migration and invasion

Wound healing assay

The detailed procedure was performed for SK-MEL-2 and MeWo cells as described in Justus, et al [24].

Cells were treated with either sterile water or inhibitors to achieve respective IC₅₀ concentrations and plates were incubated at 37°C and 5% CO₂. Photographs of wound closure were taken utilizing a Motic AE31E microscope with Moticam BTU8 Tablet (40 × magnification) at 24 h intervals for 3 days and analyzed using “ImageJ” image processing program (NIH, Rockville, MD, USA).

BME invasion assay

This *in-vitro* invasion assay was performed for SK-MEL-2 and MeWo cells as described in Feoktistova, et al. using BME (0.2 ×) as the inner coating of transwell plate [38]. Cells were treated with either sterile water or inhibitors to achieve respective IC₅₀ concentrations and plates were incubated at 37°C and 5% CO₂ for 3 days. At the end of the 3rd day, crystal violet (0.5%) was used to stain the cells adhered to the bottom surface of the membrane in transwell insert to visualize the inhibition of invasion. Photographs of the stained cells were taken from Motic AE31E microscope with Moticam BTU8 Tablet (100 × magnification) after washing the extra stains remained in the transwell plate. Subsequently, 70% Ethanol (200 µl) was added to dissolve crystal violet and absorbance was measured at 590 nm.

Immunoprecipitation and Western blot analysis

Approximately 1×10^5 cells (SK-MEL-2 and MeWo) were cultured in T75 flasks and 24 h post plating, fresh media were supplied and cells were treated with either an equal volume of sterile water or aPKC inhibitors to achieve respective IC₅₀ concentrations. Additional doses were supplied every 24 h during a 3 day incubation period. Cells were subsequently lifted and cell lysate were collected either with cell lysis buffer (C7027, Invitrogen) or IP lysis buffer (87788, Thermo Fisher). Preparation of cytosolic and nuclear extracts for the analysis of NF-κB translocation and immunoprecipitations were performed as described in Win, et al. and samples were then fractionated by SDS-PAGE and immunoblotted [12].

Immunofluorescence microscopy

SK-MEL-2 and MeWo cells were plated in chamber slides (154461, Thermo Fisher) and treated with either sterile water or inhibitors to achieve respective IC₅₀ concentrations. Slides were incubated at 37°C and 5% CO₂ for 3 days. At the end of the 3rd day, cells were prepared as described in El Bassit, et al [39]. and stained for PKC-ι (ab5282 rabbit polyclonal primary antibody 1:200 and

A21206 anti-rabbit secondary antibody at 1:1000; green) and for Vimentin (MA3-745 mouse monoclonal primary antibody at 1:40 and A32727 anti-mouse secondary antibody at 1:1000; red) to visualize under the Nikon Mirco-FX fluorescence microscope with Jenoptik D-07739 Jena camera (200 × magnification). DAPI in Gold Antifade Mountant (S36938; blue) was used to visualize the nucleus.

Inhibition of expression of PKC- ι and PKC- ζ with siRNA (RNA interference)

SK-MEL-2 and MeWo cells (4×10^4) were cultured in T25 flasks and treated with either siRNA (20 nM) for PKC- ι or PKC- ζ or scrambled siRNA after 24 h post plating time and incubated for 48 h. Detailed procedure was performed as described in Win, et al. (12).

Quantitative Real-Time PCR (qPCR)

qPCR was performed on RNA isolated from SK-MEL-2 and MeWo cell lysates collected after 3 days treatment with either an equal volume of sterile water or aPKC inhibitors with respective IC₅₀ concentrations. Expression was observed for PKC- ι using primers: Forward TTGCAATGAGGTTTCGAGACA; Reverse CTGAGATGATACTGTACACGGG. Vimentin expression was observed using primers: Forward ACACCCTGCAATCTTTCAGACA; Reverse GATTCCACTTTGCGTTCAAGGT. β -actin was used as an internal control. PCR reactions used SYBR Green PCR Mix (Applied Biosystems, CA, USA). cDNA was denatured at 95°C for 10 min, followed by 40 cycles of denaturing at 95°C for 20 s and an annealing stage of 65°C for 40 s. The Quantstudio3 was used to quantify gene expression using $\Delta\Delta$ -CT (Applied Biosystems).

Densitometry

The intensity of Western blot bands was measured using “AlphaView” software for “Fluorchem” systems developed by ProteinSimple (San Jose, CA, USA) in which the background intensity was subtracted from the intensity of each band to obtain the corrected intensity of the proteins.

Statistical analysis

All data are presented as mean \pm SD. Statistical analysis was performed with one or two-way ANOVA followed by Tukey HSD test as multiple comparisons tests using the “VassarStats” web tool for statistical analysis. P-value ≤ 0.05 or ≤ 0.01 indicated statistical significance.

Disclosure of potential conflicts of interest

No potential conflicts of interest were disclosed.

Funding

Kyrias Foundation, Brotman Foundation of California Irving S. Cooper Family Foundation Baker Hughes Foundation the Creag Foundation Bradley Zankel Foundation Frederick H. Leonhardt Foundation.


Acknowledgment

We acknowledge the generous financial contributions from the Frederick H. Leonhardt Foundation, Bradley Zankel Foundation, Inc., Kyrias Foundation, Brotman Foundation of California, Baker Hughes Foundation, Irving S. Cooper Family Foundation, and the Creag Foundation. Moreover, we thank Mrs. Rekha Patel for the assistance with fluorescence microscope experiments and Dr. Clare Dennison for allowing us to use the fluorescence microscope. We also thank Dr. Todd Sacktor for identifying ζ -Stat. Finally we thank Dr. Meera Nandjandan for her valuable suggestions on qPCR experiment designing and data interpretation.

Author contributions

W.S.R and M.A-D. conceptualization; W.S.R., C.A.A., R.J.S. and M.A.H. formal analysis; W.S.R. and M.A-D. investigation; W.S.R. and M.A-D. methodology; W.S.R. writing-original draft; W.S.R., C.A.A., A.H.A. and M.A-D. writing-review and editing; M.A-D. resources; D.A.O. and M.A-D. supervision; M. A-D. funding acquisition.

ORCID

André H. Apostolatos  <http://orcid.org/0000-0002-4527-7084>

References

- [1] Melanoma of the Skin. Cancer Stat Facts. [Internet]. [cited 2017 Oct 1]; Available from: <https://seer.cancer.gov/statfacts/html/melan.html>.
- [2] Nazarian R, Shi H, Wang Q, et al. Melanomas acquire resistance to B-RAF(V600E) inhibition by RTK or N-RAS upregulation. *Nature*. 2010;468:973–7. doi:10.1038/nature09626
- [3] Carlos G, Anforth R, Clements A, et al. Cutaneous toxic effects of BRAF inhibitors alone and in combination with MEK inhibitors for metastatic melanoma. *JAMA Dermatol*. 2015;151:1103–9. doi:10.1001/jamadermatol.2015.1745
- [4] Ascierto PA, McArthur GA, Dréno B, et al. Cobimetinib combined with vemurafenib in advanced BRAFV600-mutant melanoma (coBRIM): updated efficacy results from a randomised, double-blind, phase 3 trial. *Lancet Oncol*. 2016;17:1248–60. doi:10.1016/S1470-2045(16)30122-X

- [5] Chapman PB, Hauschild A, Robert C, et al. Improved Survival with Vemurafenib in Melanoma with BRAF V600E mutation. *N Engl J Med.* 2011;364:2507–16. doi:10.1056/NEJMoa1103782
- [6] Ratnayake WS, Apostolatos AH, Ostrov DA, et al. Two novel atypical PKC inhibitors; ACPD and DNDA effectively mitigate cell proliferation and epithelial to mesenchymal transition of metastatic melanoma while inducing apoptosis. *Int J Oncol.* 2017;51:1370–82. doi:10.3892/ijo.2017.4131
- [7] Ratnayake WS, Acevedo-Duncan M. Abstract 862: Atypical protein kinase c inhibitors can repress epithelial to mesenchymal transition (type III) in malignant melanoma. *Cancer Res.* 2017;77:862–862. doi:10.1158/1538-7445.AM2017-862
- [8] Selzer E, Okamoto I, Lucas T, et al. Protein kinase C isoforms in normal and transformed cells of the melanocytic lineage. *Melanoma Res.* 2002;12:201–9. doi:10.1097/00008390-200206000-00003
- [9] Patel R, Win H, Desai S, et al. Involvement of PKC-iota in glioma proliferation. *Cell Prolif.* 2008;41:122–35. doi:10.1111/j.1365-2184.2007.00506.x
- [10] Regala RP, Thompson EA, Fields AP. Atypical protein kinase C-L expression and aurothiomalate sensitivity in human lung cancer cells. *Cancer Res.* 2008;68:5888–95. doi:10.1158/0008-5472.CAN-08-0438
- [11] Pillai P, Desai S, Patel R, et al. A novel PKC-iota inhibitor abrogates cell proliferation and induces apoptosis in neuroblastoma. *Int J Biochem Cell Biol.* 2011;43:784–94. doi:10.1016/j.biocel.2011.02.002
- [12] Win HY, Acevedo-Duncan M. Atypical protein kinase C phosphorylates IKK alpha beta in transformed non-malignant and malignant prostate cell survival. *Cancer Lett.* 2008;270:302–11. doi:10.1016/j.canlet.2008.05.023
- [13] Stallings-Mann M, Jamieson L, Regala RP, et al. A novel small-molecule inhibitor of protein Kinase C ι blocks transformed growth of non-small-cell lung cancer cells. *Cancer Res.* 2006;66:1767–74. doi:10.1158/0008-5472.CAN-05-3405
- [14] Bensen WG, Moore N, Tugwell P, et al. HLA antigens and toxic reactions to sodium aurothiomalate in patients with rheumatoid arthritis. *J Rheumatol.* 1984;11:358–61.
- [15] Eriksson JE, He T, Trejo-Skalli AV, et al. Specific in vivo phosphorylation sites determine the assembly dynamics of vimentin intermediate filaments. *J Cell Sci.* 2004;117:919–32. doi:10.1242/jcs.00906
- [16] Zhu Q-S, Rosenblatt K, Huang K-L, et al. Vimentin is a novel AKT1 target mediating motility and invasion. *Oncogene.* 2011;30:457–70. doi:10.1038/onc.2010.421
- [17] Yasui Y, Goto H, Matsui S, et al. Protein kinases required for segregation of vimentin filaments in mitotic process. *Oncogene.* 2001;20:2868–76. doi:10.1038/sj.onc.1204407
- [18] Wang C, Shang Y, Yu J, et al. Substrate recognition mechanism of atypical protein kinase Cs revealed by the structure of PKC ι in complex with a substrate peptide from Par-3. *Structure.* 2012;20:791–801. doi:10.1016/j.str.2012.02.022
- [19] Selbie L, Schmitzpeiffer C, Sheng Y, et al. Molecular-cloning and characterization of Pkc(iota), an Atypical isoform. *J Biol Chem.* 1993;268:24296–302.
- [20] Gunaratne A, Di Guglielmo GM. Par6 is phosphorylated by aPKC to facilitate EMT. *Cell Adhes Migr.* 2013;7:357–61. doi:10.4161/cam.25651
- [21] Gunaratne A, Thai BL, Di Guglielmo GM. Atypical Protein Kinase C Phosphorylates Par6 and facilitates transforming growth factor beta-Induced Epithelial-to-Mesenchymal transition. *Mol Cell Biol.* 2013;33:874–86. doi:10.1128/MCB.00837-12
- [22] Scott M, Fujita T, Liou H, et al. The P65-Subunit of Nf-Kappa-B regulates I-Kappa-B by 2 distinct mechanisms. *Genes Dev.* 1993;7:1266–76. doi:10.1101/gad.7.7a.1266
- [23] Lamouille S, Xu J, Derynck R. Molecular mechanisms of epithelial-mesenchymal transition. *Nat Rev Mol Cell Biol.* 2014;15:178–96. doi:10.1038/nrm3758
- [24] Justus CR, Leffler N, Ruiz-Echevarria M, et al. In vitro cell migration and invasion assays. *J Vis Exp JoVE.* 2014;88:51046. <https://www.ncbi.nlm.nih.gov/pmc/articles/PMC4186330/> doi:10.3791/51046.
- [25] Valcourt U, Kowanetz M, Niimi H, et al. TGF-beta and the Smad signaling pathway support transcriptomic reprogramming during epithelial-mesenchymal cell transition. *Mol Biol Cell.* 2005;16:1987–2002. doi:10.1091/mbc.e04-08-0658
- [26] Nelson WJ. Remodeling epithelial cell organization: Transitions between front-rear and apical-basal polarity. *Cold Spring Harb Perspect Biol.* [Internet] 2009;1:a000513. <https://www.ncbi.nlm.nih.gov/pmc/articles/PMC2742086/>.
- [27] Apostolatos AH, Ratnayake WS, Smalley T, et al. Abstract 2369: Transcription activators that regulate PKC-iota expression and are downstream targets of PKC-iota. *Cancer Res.* 2017;77:2369–2369. doi:10.1158/1538-7445.AM2017-2369
- [28] Inagaki M, Inagaki N, Takahashi T, et al. Phosphorylation-dependent control of structures of intermediate filaments: A novel approach using site- and phosphorylation state-specific antibodies. *J Biochem (Tokyo).* 1997;121:407–14. doi:10.1093/oxfordjournals.jbchem.a021603
- [29] Kourtidis A, Ngok SP, Anastasiadis PZ. p120 catenin: an essential regulator of cadherin stability, adhesion-induced signaling, and cancer progression. *Prog Mol Biol Transl Sci.* 2013;116:409–32. doi:10.1016/B978-0-12-394311-8.00018-2
- [30] Koenig A, Mueller C, Hasel C, et al. Collagen Type I Induces Disruption of E-Cadherin-mediated cell-cell contacts and promotes proliferation of pancreatic carcinoma cells. *Cancer Res.* 2006;66:4662–71. doi:10.1158/0008-5472.CAN-05-2804
- [31] Kasof GM, Lu JJ, Liu DR, et al. Tumor necrosis factor-alpha induces the expression of DR6, a member of the TNF receptor family, through activation of NF-kappa B. *Oncogene.* 2001;20:7965–75. doi:10.1038/sj.onc.1204985
- [32] Yook JI, Li X-Y, Ota I, et al. A Wnt-Axin2-GSK3beta cascade regulates Snail1 activity in breast cancer cells. *Nat Cell Biol.* 2006;8:1398–406. doi:10.1038/ncb1508
- [33] Sahlgren C, Gustafsson MV, Jin S, et al. Notch signaling mediates hypoxia-induced tumor cell migration and invasion. *Proc Natl Acad Sci.* 2008;105:6392–7. doi:10.1073/pnas.0802047105
- [34] Wu Y, Deng J, Rychahou PG, et al. Stabilization of snail by NF- κ B is required for inflammation-induced cell

- migration and invasion. *Cancer Cell*. 2009;15:416–28. doi:10.1016/j.ccr.2009.03.016
- [35] Xi G, Shen X, Rosen CJ, et al. IRS-1 functions as a molecular scaffold to coordinate IGF-I/IGFBP-2 signaling during osteoblast differentiation. *J Bone Miner Res*. 2016;31:1300–14. doi:10.1002/jbmr.2791
- [36] Trott O, Olson AJ. AutoDock Vina: improving the speed and accuracy of docking with a new scoring function, efficient optimization and multithreading. *J Comput Chem*. 2010;31:455–61.
- [37] Weininger D. SMILES, a chemical language and information system. 1. Introduction to methodology and encoding rules. *J Chem Inf Comput Sci*. 1988;28:31–6. doi:10.1021/ci00057a005
- [38] Feoktistova M, Geserick P, Leverkus M. Crystal violet assay for determining viability of cultured cells. *Cold Spring Harb Protoc*. 2016;2016:pdb.prot087379. doi:10.1101/pdb.prot087379
- [39] El Bassit G, Patel RS, Carter G, et al. MALAT1 in human adipose stem cells modulates survival and alternative splicing of PKC δ II in HT22 cells. *Endocrinology*. 2017;158:183–95.
- [40] Chaw SY, Abdul Majeed A, Dalley AJ, et al. Epithelial to mesenchymal transition (EMT) biomarkers – E-cadherin, beta-catenin, APC and Vimentin – in oral squamous cell carcinogenesis and transformation. *Oral Oncol*. 2012;48:997–1006. doi:10.1016/j.oraloncology.2012.05.011